27 November 1998

ELSEVIER

Chemical Physics Letters 297 (1998) 321–328

CHEMICAL PHYSICS LETTERS

Valence electron distribution in $La_2Li_{1/2}Cu_{1/2}O_4$, $Nd_2Li_{1/2}Ni_{1/2}O_4$, and $La_2Li_{1/2}Co_{1/2}O_4$

Z. Hu [a], Chandan Mazumdar [a], G. Kaindl [a,*], F.M.F. de Groot [b], S.A. Warda [c], D. Reinen [c]

[a] *Institut für Experimentalphysik, Freie Universität Berlin, Arnimallee 14, D-14195 Berlin-Dahlem, Germany*
[b] *Solid-State Physics, University of Groningen, Nijenborgh 4, NL-9747 AG Groningen, The Netherlands*
[c] *Fachbereich Chemie und Zentrum für Materialwissenschaften, Philipps-Universität Marburg, Lahnberge, D-35032 Marburg, Germany*

Received 19 June 1998; in final form 5 October 1998

Abstract

The distribution of valence electrons between transition metals (TM) and oxygen has been studied via X-ray absorption near-edge fine structure (XANES) at the TM-$L_{2,3}$ and O-K thresholds for $La_2Li_{1/2}Cu_{1/2}O_4$, $Nd_2Li_{1/2}Ni_{1/2}O_4$, and $La_2Li_{1/2}Co_{1/2}O_4$. Simulations of the TM-$L_{2,3}$ XANES by charge-transfer multiplet calculations result in 3d-hole concentrations that increase from $\sim 30\%$ $3d^8$ in the Cu(III) to $\sim 57\%$ $3d^7$ in the Ni(III) to $\sim 72\%$ $3d^6$ in the Co(III) compound. Concomitantly, the O-K XANES spectra reflect an increase of bond ionicity in the same sequence. The results show that the Li-doped holes in $Nd_2Li_{1/2}Ni_{1/2}O_4$ are distributed between Ni-3d and O-2p orbitals.

1. Introduction

High-energy spectroscopies form a powerful tool for studying the electronic structure of 3d transition-metal (TM) oxides, since the spectral features are rather sensitive to changes in the correlation of the TM 3d electrons as well as the TM-3d/O-2p covalence. Ever since the discovery of high-T_c superconductivity in the cuprates, Sr- and Li-doped 3d-TM oxides have been an important issue in such high-energy spectroscopies [1]. In systems like $La_{2-x}Sr_xMO_4$ (M = Cu, Ni) and $Li_xNi_{1-x}O$, where the oxidation states of Cu and Ni are higher than $2+$, it was usually concluded on the basis of X-ray absorption near-edge structure (XANES) and core-level photoemission (XPS) spectra that Sr- and Li-doping induces holes in the O-2p band [2–8]. Contributions of $3d^8$ in the case of Cu(III) and $3d^7$ in the case of Ni(III) compounds to the ground-state wavefunctions were only hesitantly admitted. This went as far as postulating an $\alpha|3d^9\rangle + \beta|3d^9\underline{L}\rangle$ ground state for $La_2Li_{1/2}Cu_{1/2}O_{4-\delta}$ (with $\alpha^2 + \beta^2 = 1$; $\underline{L}$ refers to a hole in the O-2p orbitals; δ = oxygen deficit) and excluding the existence of a contribution from a $3d^8$ configuration to the ground state [9].

The solids $La_2(Nd_2)Li_{1/2}TM_{1/2}O_4$ [TM(III) = Cu, Ni, Co] crystallize in a variant of the K_2NiF_4 structure, with an ordered distribution of the TM ions

* Corresponding author. E-mail: kaindl@physik.fu-berlin.de

0009-2614/98/$ - see front matter
PII: S0009-2614(98)01135-X

and lithium(I) over the octahedral sites [10]. This structure has the advantage that the TMO_6 polyhedra are isolated in the lattice and can be studied spectroscopically without being disturbed by intercluster interactions. Recent magnetic measurements and electron paramagnetic resonance (EPR) studies showed that at room temperature the ground state of Cu(III), Ni(III), and Co(III) in these compounds is low spin, however, with closeby excited high-spin states in the latter case [10]. The existence of a mixed-spin or a high-spin state for Co(III), suggested from earlier magnetic results in Refs. [11,12], could not be confirmed in this work. In order to clarify further the electronic structure of the late 3d-TM(III) oxides, we have measured XANES spectra of $La_2Li_{1/2}TM_{1/2}O_4$ (TM = Cu, Co) and Nd_2-$Li_{1/2}Ni_{1/2}O_4$ at the TM-$L_{2,3}$ and O-K thresholds; in the Ni compound, La was replaced by Nd due to an energy overlap of the La-$3d_{3/2}$ and Ni-$2p_{3/2}$ thresholds.

With respect to theory, the $L_{2,3}$ XANES spectra of 3d-TM compounds have been reproduced successfully by atomic-multiplet calculations in previous work [13]. However, many-body interactions induced by covalence become important for Cu(III) and Ni(III) oxides, i.e. atomic-multiplet calculations are no longer valid here. Considering the effects of covalence, a charge-transfer program has been combined with the atomic-multiplet program used in Ref. [13]. Making use of this, we were able to simulate the experimental spectra in more detail, obtaining in this way information on the distribution of holes induced by Li-doping between the TM-3d and O-2p orbitals in the ground state.

2. Experimental

The solids $La_2(Nd_2)Li_{1/2}TM_{1/2}O_4$ (TM = Cu, Ni, Co) were prepared according to the procedures described in Ref. [10]. The purity of the compounds was checked by single-crystal X-ray analysis and iodometric determination of the oxidation states of nickel and copper: in addition, supplementary optical and EPR-spectroscopic investigations were performed [10]. The XANES measurements were carried out using the SX700/II monochromator operated by the Freie Universität Berlin at the Berliner Elektronenspeicherring für Synchrotronstrahlung (BESSY). For the O-K XANES studies, the fluorescence-yield mode was used, whereas the TM-$L_{2,3}$ spectra were recorded via the total-electron yield. At the O-K and Cu-L_3 threshold, the experimental resolution (full width at half maximum) was 0.3 and 0.5 eV, respectively. The samples were stored and transferred in a clean Ar atmosphere to the experimental ultra-high vacuum (UHV) chamber, which had a base pressure of $< 1 \times 10^{-10}$ mbar.

Since all of the studied oxides are insulators, the samples charged up during the measurements, which, however, does not influence the XANES spectra directly. Furthermore, the Cu(III) and Ni(III) compounds were found not to be stable enough in order to fully exclude a decomposition of the sample surfaces when exposed to an intense X-ray beam in the UHV. In this way, an oxygen deficiency might form on the sample surface. By restricting the data-taking periods to a few minutes after each cleaning cycle, we kept such effects on the TM-$L_{2,3}$ XANES spectra, recorded in the total-electron-yield mode, to a minimum. Even though the counting times were slightly longer in the case of the O-K XANES spectra taken via fluorescence yield ($\sim$ 20 min), the effects of surface impurities were smaller due to a much higher volume sensitivity (sampling depth: $\sim$ 1000 Å in fluorescence yield as compared to $\sim$ 30 Å in total-electron yield). Furthermore, we know from our previous study of $NaCuO_2$ that the spectral features in the Cu-$L_{2,3}$ XANES spectrum are quite sensitive to the formation of a surface Cu(II) impurity phase, which can be distinguished from CuO on the basis of the energies of the related peaks [14].

3. Results and discussion

The Cu-$L_{2,3}$ XANES spectrum of $La_2Li_{1/2}$-$Cu_{1/2}O_4$ is shown in Fig. 1 (top panel); it is very similar to that of $NaCuO_2$ [14], where the main peak and the satellite ($\sim$ 8.5 eV above the main peak) were basically assigned to $\underline{2p}3d^{10}\underline{L}$ and $\underline{2p}3d^9$ final states, respectively ($\underline{2p}$ refers to the core hole). The weak shoulder at 1.7 eV below the main peak, which

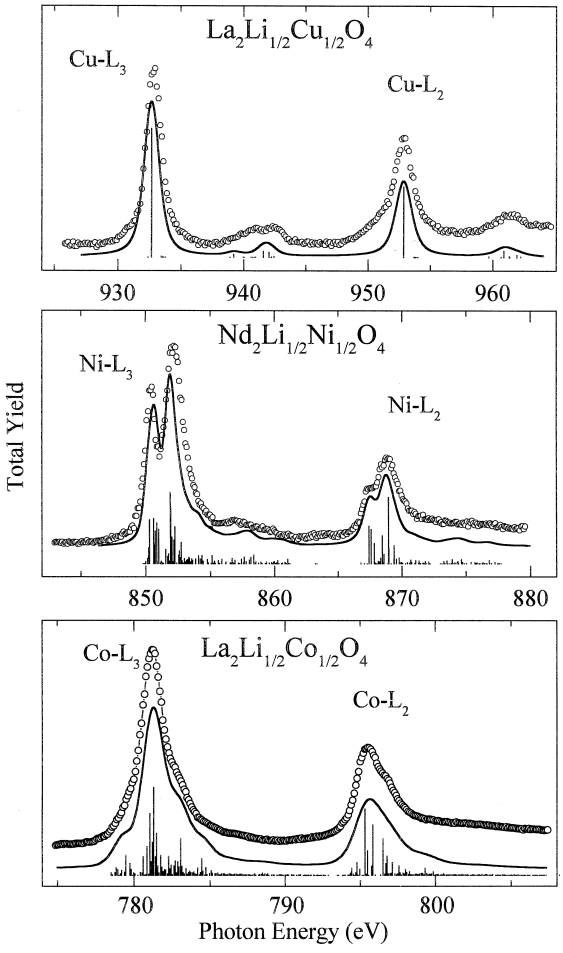

Fig. 1. Cu-$L_{2,3}$ (top), Ni-$L_{2,3}$ (center), and Co-$L_{2,3}$ (bottom) XANES spectra of $La_2Li_{1/2}Cu_{1/2}O_4$, $Nd_2Li_{1/2}Ni_{1/2}O_4$, and $La_2Li_{1/2}Co_{1/2}O_4$, recorded in the total-electron-yield mode (open circles). For comparison, the results of charge-transfer multiplet calculations are also given (solid curves and bar diagrams).

had been observed in case of $NaCuO_2$, is nearly missing in the spectrum of $La_2Li_{1/2}Cu_{1/2}O_4$. Since this shoulder is at the same energy as the main peak in the spectrum of CuO, we assign it to a Cu(II) impurity. In this way, we can rule out a $3d^9$ configuration in $La_2Li_{1/2}Cu_{1/2}O_4$ and confirm the 3+ oxidation state of copper.

The core-level spectra of such strongly correlated systems can be described in a many-body scheme. In Eqs. (1) and (2), we define the Hamiltonian for a $3d^n$ system and the corresponding ground-state wavefunction, where – for simplicity – mixing with a $d^{n+2}\underline{L}^2$ configuration has been neglected:

$$H = \begin{vmatrix} 0 & T \\ T & U \end{vmatrix} \tag{1}$$

$$\Phi_g = \alpha_0 |3d^n\rangle + \beta_0 |3d^{n+1}\underline{L}\rangle , \tag{2}$$

with

$$\left(\alpha_0^2 + \beta_0^2\right) = 1 .$$

$U = \Delta$ denotes the charge-transfer energy, T is the $3d \rightarrow \underline{L}$ charge-transfer integral, and $n = 8, 7, 6$ for Cu(III), Ni(III), Co(III), respectively. The configuration-mixing coefficients α_0 and β_0 in the ground state are related to each other in the following way:

$$\beta_0/\alpha_0 = \left\{\left(\Delta^2 + 4T^2\right)^{1/2} - \Delta\right\}/2T . \tag{3}$$

When going from Cu(II) to Cu(III) oxides, Δ decreases significantly, even becoming negative for $NaCuO_2$ ($\Delta = -2.5$ eV) [5]. From Eq. (3), a β_0/α_0 ratio larger than 1 is obtained, implying $3d^9\underline{L}$ as the dominant contribution to the ground state of this Cu(III) oxide. The schematic energies of the $L_{2,3}$-XANES final states and configuration-mixing coefficients α and β are given by Eqs. (4)–(8)

$$H = \begin{vmatrix} 0 & T_f \\ T_f & U_f \end{vmatrix} , \tag{4}$$

$$\Phi_m = \alpha |\underline{2p}3d^{n+1}\rangle + \beta |\underline{2p}3d^{n+2}\underline{L}\rangle , \tag{5}$$

$$\Phi_s = \beta |\underline{2p}3d^{n+1}\rangle - \alpha |\underline{2p}3d^{n+2}\underline{L}\rangle , \tag{6}$$

$$E_{m/s} = 1/2\left\{\left(U_f^2 + 4T_f^2\right)^{1/2} \mp U_f\right\} , \tag{7}$$

$$\beta/\alpha = \left\{\left(U_f^2 + 4T_f^2\right)^{1/2} - U_f\right\}/2T_f . \tag{8}$$

Here, T_f is the $d \rightarrow \underline{L}$ transfer integral in the final state, and U_f is equal to $\Delta - U_{cd} + U_{dd}$, where U_{cd} and U_{dd} denote the Cu-2p core-hole/3d and 3d/3d Coulomb interactions, respectively. Φ_m and Φ_s, as well as the corresponding energy $E_{m/s}$, refer to the main peak and the satellite, respectively. The intensity distribution between the satellite and the main peak is determined by the degree of covalent mixing in the ground state as well as by the interference effect in the final state, as described by Eq. (9):

$$I_s/I_m \sim \left(\alpha_0\beta - \beta_0\alpha\right)^2/\left(\alpha_0\alpha + \beta_0\beta\right)^2 . \tag{9}$$

From Eq. (9), one deduces a weak intensity of the satellite, however, this does not necessarily mean that the $3d^8$ contribution to the ground state is that small. For $T_f = T$ and $U_{cd} = U_{dd}$, the intensity of the satellite could even be fully transferred to the main peak. Since we know from energy estimates that $-U_{cd} + U_{dd} \sim -2$ eV [5], U_f is more negative than Δ, which means that for $La_2Li_{1/2}Cu_{1/2}O_4$ one expects the $\underline{2p}3d^{10}\underline{L}$ contribution to the final state in the $L_{2,3}$-XANES spectrum (main peak) to be larger than the $3d^9\underline{L}$ fraction in the ground state. Thus the main peak and the satellite in the $L_{2,3}$-XANES spectra of Cu(III) oxides can be assigned to the $\underline{2p}3d^{10}\underline{L}$ and $\underline{2p}3d^9$ final states, respectively [14].

The Ni(III) centers have a low-spin electron configuration, which means that the single electron beyond the closed d^6 configuration resides in an e_g orbital. The Ni-$L_{2,3}$ XANES spectrum of $Nd_2Li_{1/2}Ni_{1/2}O_4$ is displayed in Fig. 1 (center panel). At the L_3 threshold a double-peaked structure, with a dominant peak at higher energy, is observed. This is quite unique for Ni compounds; in addition, a broad satellite structure is found above the main peak, analogous to $La_2Li_{1/2}Cu_{1/2}O_4$. The multiplet is more complex than that of the analogous copper system because final states with more than one hole in the 3d shell are subject to an extended multiplet structure due to inter-electronic Coulomb interaction [13]. The two main peaks in the L_3 spectrum are 0.4 and 2.1 eV, respectively, above the dominant peak in the spectrum of NiO (not presented here). Without details of a theoretical description, it is practically not possible to give an assignment of the observed spectral features.

At room temperature, the Co(III) centers in $LaCoO_3$ are in a low-spin state, and a transition to a high-spin state above room temperature has been observed by XANES studies [15], which did not confirm the earlier Mössbauer results claiming the occurrence of a mixed-spin state at 200 K [16]. The Co-$L_{2,3}$ XANES spectrum of $La_2Li_{1/2}Co_{1/2}O_4$ (Fig. 1, bottom panel) is very similar to that of low-spin $LaCoO_3$ and $LiCoO_2$ recorded at 300 K [15,17]; we therefore assign it to a low-spin state, with filled t_{2g} and empty e_g orbitals, stabilizing ionic trivalent Co. The difference between $La_2Li_{1/2}Co_{1/2}O_4$ and $LaCuO_3$ and $LiCoO_2$ is in the weak structure at the leading edge of the main peak (at $\sim$ 779 eV), which is very weak in $La_2Li_{1/2}Co_{1/2}O_4$ after proper scraping, showing that it is at least partly due to a Co(II) impurity. The combined effects of mixed spin and strong covalence in Co(III) compounds has led in the past to difficulties in theoretically reproducing the experimental multiplet structures [15,17]. As shown in the following section, the charge-transfer multiplet calculations of the present work are well suited for reproducing the experimental spectra in more detail.

4. Results of charge-transfer multiplet calculations

In order to derive $3d^n$ weights in the ground state from the spectra, we have performed charge-transfer multiplet calculations using our TT-MULTIPLETS program, which consists of a package of programs including parts of the atomic-multiplet program of Cowan [18], the group-theory program of Butler [19], and the charge-transfer program of Okada et al. [20]. In the actual calculations, the dimensions of the various multiplet states must be used, these being 45 for $3d^8$ and 60 for $3d^9\underline{L}$ (reduced by symmetry). The matrix in Eq. (1) consists of 45×45 and 60×60 diagonal blocks mixed together by hopping. Depending on the assumed symmetry, the actual matrices are smaller. The D_{4h} symmetry of the strongly elongated CuO_6 polyhedron in $La_2Li_{1/2}Cu_{1/2}O_4$ is described by an (ionic) tetragonal crystal field, with 10 Dq = 0.5 eV and Ds = 0.3 eV. The mixing terms are separated into four symmetries, A_{1g}, B_{1g}, A_{2g}, and E_g, using the relations between these as described by Eskes et al. [21]. The mixing terms are 3.0, 1.73, 1.5, and 1.03 eV in the case of A_{1g}, B_{1g}, A_{1g}, and E_g, respectively. The resulting many-electron ground state is $^1A_{1g}$, with both holes in the $x^2 - y^2$ orbital (low spin).

The top panel in Fig. 1 gives a comparison between theory (solid curve) and experiment (open dots) for $La_2Li_{1/2}Cu_{1/2}O_4$. The vertical bars represent the energies and intensities resulting from the calculation, while the solid curve represents the spectrum obtained by inclusion of a Lorentzian life-time broadening of 0.6 eV at L_3 (0.90 eV at L_2), plus an experimental Gaussian broadening of 0.6 eV (FWHM). All structures observed experimentally are well reproduced in the calculation, in particular the

sharp main peak and the poorly resolved double-peaked structure at ~941 eV. The main peak is dominated by $\underline{2p}3d^{10}\underline{L}$ character, whereas the double-peaked satellite relates to a $\underline{2p}3d^9$-dominated final state, displaying a multiplet structure, which is formed by a combination of multiplet ($\underline{2p}$-3d interaction), crystal-field, and charge-transfer effects. The position and intensity of this structure with respect to the main peak essentially determines the amount of mixing and the separation of the peaks; this sets limits to the values of Δ as well as to the hopping. The comparison shows that the spectrum of $La_2Li_{1/2}Cu_{1/2}O_4$ can be simulated by using $U_{cd} - U_{dd} = 2$ eV and $\Delta = -1.9$ eV. Following the literature [20,21], Δ is defined as the energy difference between the lowest $3d^8$ and the lowest $3d^9\underline{L}$ state. The multiplet calculations require as an input parameter the energy difference Δ(average) between the centers-of-gravity of the $3d^8$ and $3d^9\underline{L}$ configurations, which is equal to -3.0 eV. The percentage of $3d^8$ character was found to be 30% in the ground state (see Table 1).

The theoretical Ni-$L_{2,3}$ XANES spectrum of $Nd_2Li_{1/2}Ni_{1/2}O_4$ (solid curve in center panel of Fig. 1) was calculated using a Δ value of $+0.5$ eV (related to a Δ(average) value of -1.0 eV). The mixing parameters are equal to those of $La_2Li_{1/2}Cu_{1/2}O_4$, because the MO_6 polyhedra (M = Cu, Ni) have similar geometries [10]. Also, the ionic crystal-field values have been set equal (10 Dq = 0.5 eV; Ds = 0.3 eV). These values determine the Ni(III) ground state as low spin, $^2A_{1g}$, approximately related to two holes in the $x^2 - y^2$ orbital, with the third hole in the z^2 state. Because Δ is close to zero, the ground state – according to Eq. (3) – contains almost equal amounts of $3d^7$ and $3d^8\underline{L}$; the actual percentage of $3d^7$ is 57%. This strongly intermixed ground state makes it doubtful to assign a particular final-state configuration to a particular peak. It is best to say that the whole spectral shape is given by strongly mixed $\underline{2p}3d^8$ and $\underline{2p}3d^9\underline{L}$ states. The theoretical simulation clearly proves the low-spin nature of Ni(III) in case of $Nd_2Li_{1/2}Ni_{1/2}O_4$, with an $^2A_{1g}$ ground state due to tetragonally elongated Ni(III)O_6 octahedra as the consequence of vibronic Jahn–Teller coupling, in agreement with the spectral shape as well as the recent structural and EPR results [10], with 57% $3d^7$ and 43% $3d^8\underline{L}$ character (see Table 1).

In order to understand further the effects of covalence on Co(III) XANES spectra, we have calculated theoretical spectra for various values of Δ and 10 Dq. The best agreement with the experimental spectrum of $La_2Li_{1/2}Co_{1/2}O_4$ was obtained for $\Delta = 3.5$ eV and 10 Dq = 1.6 eV, with $U_{cd} - U_{dd} = 2$ eV; the results are shown by the solid curve in Fig. 1 (bottom panel). This represents a low-spin ground state of Co(III) in $La_2Li_{1/2}Co_{1/2}O_4$, consistent with previous studies of $LiCoO_2$ and $LaCoO_3$ [15,17]. The ground state of Co(III) contains ~72% $3d^6$, i.e. $La_2Li_{1/2}Co_{1/2}O_4$ contains the most ionic trivalent TM in this series of compounds (see Table 1). There is a first excited state at ~28 meV with an $S = 2$ high-spin character. Applying Boltzmann statistics leads to a change in the spectral shape as a function of temperature over the range of, for example, 200–500 K as the excited state gets populated. Such effects have been observed in case of $LaCoO_3$ by Abbate et al. [15]. Note also that other effects, such as changes of the crystal field, may contribute to the temperature dependence but it is interesting to note that a simple population effect may be sufficient.

The variation in the distribution of holes between TM-3d and O-2p in the studied series of compounds is attributed to differences in the relative magnitudes of the Mott–Hubbard energy, U (required to transfer a 3d electron from one TM ion to a neighboring one), and the charge-transfer energy, Δ. According to the Zaanen–Sawatzky–Allen (ZSA) classification scheme [23], a Mott–Hubbard insulator requires $\Delta > U$, while $U > \Delta$ leads to a charge-transfer insulator. Table 1 summarizes the occupation numbers in the ground state obtained for the studied compounds,

Table 1
Weights of $3d^n$ and $3d^{n+1}\underline{L}$ configurations, charge-transfer energy, Δ, and Coulomb repulsion energy, U, for the ground states of the compounds $La_2(Nd_2)Li_{1/2}TM_{1/2}O_4$

Compound	Δ (eV)	U (eV)	$3d^n$ (%)	10 Dq (eV)
$La_2Li_{1/2}Co_{1/2}O_4$	3.5	5.0[a]	72	1.6
$Nd_2Li_{1/2}Ni_{1/2}O_4$	0.5	6.7[b]	57	0.5
$La_2Li_{1/2}Cu_{1/2}O_4$	−1.9	6.5[c]	30	0.5

[a] Ref. [15].
[b] Ref. [6].
[c] Ref. [5].

as well as values for Δ and U taken from previous work [5,6,15]. A comparison of Δ with U shows that $Nd_2Li_{1/2}Ni_{1/2}O_4$ falls into the charge-transfer region with a smaller p–d gap, whereas $La_2Li_{1/2}Co_{1/2}O_4$ has intermediate properties. In case of $La_2Li_{1/2}Cu_{1/2}O_4$, Δ is negative, i.e. this compound has a p–p band gap outside the ZSA scheme (similar to $NaCuO_2$ [5]).

At this point we want to compare $Nd_2Li_{1/2}Ni_{1/2}O_4$ with $Li_xNi_{1-x}O$. In the latter system, the Li ions are statistically distributed over the rock-salt lattice, and Li-doped holes are bound to Li^+ impurities [6,7]. In the former compound, Li is only a counter ion, with holes being restricted to isolated NiO_6 clusters. It has become clear that non-local contributions arise when the metal polyhedra in the lattice are not isolated, but rather interconnected by shared ligand atoms resulting in charge transfer from remote ligands to 3d-TM ions [20,24]. As a consequence, pronounced shifts of the charge-transfer bands to lower energies have been observed, enhancing the apparent covalent effects [20,24,22]. Non-local effects in $Nd_2Li_{1/2}Ni_{1/2}O_4$ can be neglected on the basis of structural arguments, i.e. we have observed by high-energy spectroscopy large $3d^7$ weights in the ground state of isolated NiO_6 clusters.

In O-K XANES spectra, correlation effects are much weaker than in 3d TM-$L_{2,3}$ XANES spectra, i.e. the good agreement between the experimental spectra and the results of band-structure calculations is plausible [17,25,26]. Therefore, O-K XANES spectra are usually studied in order to explore the amount of O-2p holes induced by covalence in the ground state. Fig. 2 displays the O-K XANES spectra of the three oxides studied. We can divide the spectra into two regions: in the first region, a narrow pre-edge peak is observed for all three compounds, which is assigned to the hole fraction with O-2p character in the e_g orbitals caused by TM-3d/O-2p mixing. In the second region from $\sim$ 532 to 539 eV, a broader structure sitting on the edge jump is observed and this is attributed to Ln-5d bands [15,17,26]. Since only intra-atomic transition-matrix elements are allowed, according to Eq. (1), the pre-edge peak is assigned to a $\underline{1s}3d^{n+1}$ final state, with a spectral weight proportional to β_0^2 [7]. The spectral intensity of the pre-edge peak, I_1, is scaled with $k = 4/(I_2 * \underline{n})$, where I_2 is the spectral weight in the second region and $\underline{n} = 2, 3, 4$ for Cu, Ni, Co, respectively (referring to the number of 3d holes).

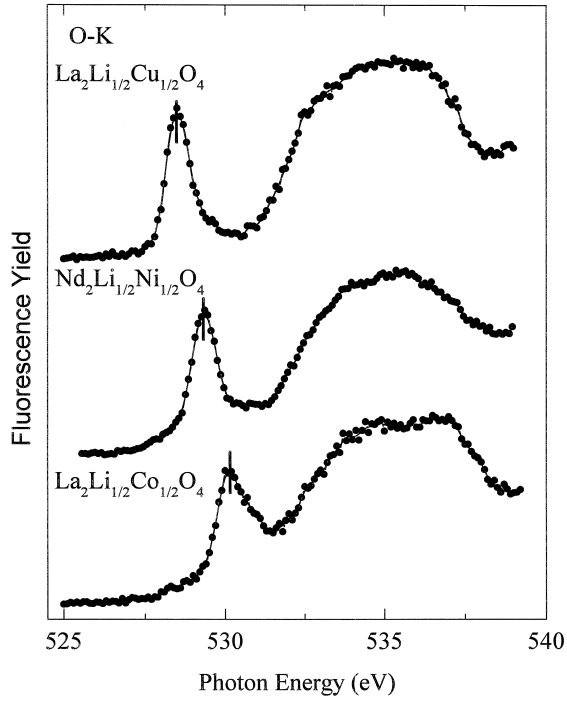

Fig. 2. O-K XANES spectra of $La_2(Nd_2)Li_{1/2}TM_{1/2}O_4$ for TM = Cu, Ni, Co.

The results for kI_1 are shown in Fig. 3 (open circles) together with β_0^2 derived from the TM-$L_{2,3}$ XANES spectra (filled squares). A similar behavior is found on the basis of core-level spectra at both TM and O sites. Recently, band-structure calculations in local-density approximation for $La_2Li_{1/2}Cu_{1/2}O_4$ have shown that the localized hole, originating from isolated CuO_4 clusters, is responsible for the insulating properties of this compound [27]. A bandwidth of $\sim$ 0.9 eV was obtained theoretically. The total experimental width of the pre-edge peak is 0.9 eV. Subtracting 0.4 eV for the combined effect of the finite experimental resolution and lifetime broadening, a bandwidth of 0.5 eV is obtained. This means that this band is even more localized than predicted theoretically, where core-hole effects have not been included. We thus conclude that the first unoccupied state in $La_2Li_{1/2}Cu_{1/2}O_4$ is more strongly localized than the O-2p holes induced by out-of-plane Sr substitution of La in $La_{2-x}Sr_xCuO_4$,

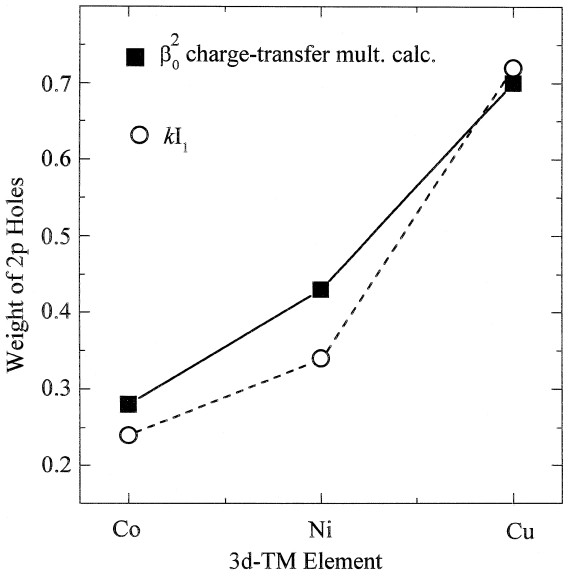

Fig. 3. Weights β_0^2 of 3d holes in the ground states of $La_2(Nd_2)Li_{1/2}TM_{1/2}O_4$ for TM = Cu, Ni, Co, as derived from charge-transfer multiplet calculations. For comparison, the spectral intensities of the pre-edge peak, I_1, scaled by $k = 4/(\underline{n}I_2)$, are also plotted; here, I_2 refer to the spectral weights of the second regions, and $\underline{n} = 2, 3, 4$ are numbers of formal 3d holes in the studied compounds for Cu, Ni, Co, respectively.

since the linewidth of the pre-edge peak in the O-K XANES spectrum of $La_{2-x}Sr_xCuO_4$ is broader than that in $La_2Li_{1/2}Cu_{1/2}O_4$ [4,8,28]. Note that there is clearly no structure observed at ~ 530.3 eV (the energy of the main peak in the spectrum of CuO), excluding again a $3d^9$ configuration in the ground state of the Cu(III) compound studied. From the point of view of Li doping, one can say that the $3d^9$ states transfer totally to the doped-hole states.

The pre-edge peak ($1\underline{s}3d^8$ final state) in the O-K XANES spectrum of $Nd_2Li_{1/2}Ni_{1/2}O_4$ lies 2.6 eV below the $1\underline{s}3d^9$ final state at 531.9 eV in NiO. Since the latter state overlaps in energy with the broad peak (between 532 and 537 eV) in the spectrum of $Nd_2Li_{1/2}Ni_{1/2}O_4$, which is due to transition into band states mainly of Nd5d character, we cannot rule out a Ni(II) impurity, which would give rise to a $1\underline{s}3d^9$ signal. However, the intensity at this energy is significantly lower than in La_2NiO_4 [4], and even weaker than in $La_{0.9}Sr_{1.1}NiO_4$ [2]. Note that substitution of La by Sr in $La_{2-x}Sr_xNiO_4$, which is out of plane, introduces further mobile holes and a sharing of corners of the NiO_6 clusters, resulting in an enhancement of covalence by non-local effects. This is reflected in a broader and weaker pre-edge peak and a larger spectral weight of the $1\underline{s}3d^9$ state [24,22]. We should also point out that the O-K XANES spectrum of $La_2Li_{1/2}Co_{1/2}O_4$ is very similar to that of $LaCoO_3$ studied before at room temperature; this further confirms the low-spin nature of Co(III) in this compound at room temperature [15].

The pre-edge peak shifts by -0.7 eV from Co to Ni, and further by -0.8 eV from Ni to Cu, in accordance with Sugiura et al., who observed a systematic shift of the pre-edge peak to lower energy when the ionization potential of the metal ion in the same oxidation state increases [29,30]. Indeed, the third ionization potential is 33.5 eV for Co, 35.17 eV for Ni, and 36.84 eV for Cu [18]. This trend predicts a decrease of the gap from Co(III) to Ni(III) and further to Cu(III), as is indeed observed. On the basis of these arguments, we can also understand the more pronounced metallic properties of $La_{2-x}Sr_xMO_4$ materials for TM = Cu as compared to TM = Ni.

5. Summary and conclusions

The electronic structures of the trivalent 3d-TM oxides $La_2(Nd_2)Li_{1/2}TM_{1/2}O_4$ (TM = Cu, Ni, Co) were described on the basis of covalent mixing between $3d^n$ and $3d^{n+1}\underline{L}$ states. The TM-$L_{2,3}$ XANES spectra were successfully reproduced by charge-transfer multiplet calculations providing quantitative results on the distribution of holes between the TM-3d and the O-2p states. The ionicity (covalence) increases (decreases) from Cu(III) to Ni(III) and further to Co(III) in this series of compounds. The pre-edge peak in the O-K XANES spectra of the oxides studied shifts systematically to higher energies in the same sequence, indicating an increase of the band gap. The cation order between Li(I) and TM(III) in the solids $Ln_2Li_{1/2}TM_{1/2}O_4$ results in isolated TMO_6 clusters and localized hole states in the band gap, i.e. insulating behavior. In contrast, the interconnection between the TMO_6 polyhedra and the mixed-valence behavior in the mixed crystals $Ln_{2-x}Sr_xTMO_4$ leads to more mobile holes and extended electron delocalization. In this

way, we can understand the significant differences between $Nd_2Li_{1/2}Ni_{1/2}O_4$ and the previously studied $Li_xNi_{1-x}O$ and $La_{2-x}Sr_xNiO_4$ systems.

Acknowledgements

This work was supported by the Deutsche Forschungsgemeinschaft, Projects Ka 564/7-1 and Re 164/32-2, as well as the Bundesminister für Bildung, Wissenschaft, Forschung und Technologie, Project 05-621 KEB. CM thanks the Alexander-von-Humboldt-Stiftung for financial support. The research of FdG has been made possible by the Royal Netherlands Academy of Arts and Sciences (KNAW).

References

[1] M. Khairy, P. Odier, J. Choisnet, J. Phys. Collog. C1 47 (1986) 831.
[2] P. Kuiper, J. van Elp, G.A. Sawatzky, A. Fujimori, S. Hosoya, D.M. de Leeuw, Phys. Rev. B 44 (1991) 4570.
[3] H. Eisaki, S. Uchida, T. Mizokawa, H. Namatame, A. Fujimori, J. van Elp, P. Kuiper, G.A. Sawatzky, S. Hosoya, H. Katayama-Yoshida, Phys. Rev. B 45 (1992) 12513.
[4] E. Pellegrin, C.T. Chen, J. Zaanan, J. Fink, Physica B 208,209 (1995) 487.
[5] T. Mizokawa, A. Fujimori, H. Namatame, K. Akeyama, N. Kosugi, Phys. Rev. B 49 (1994) 7193.
[6] J. van Elp, H. Eskes, P. Kuiper, G.A. Sawatzky, Phys. Rev. B 45 (1992) 1612.
[7] P. Kuiper, G. Kruizinga, J. Ghijsen, G.A. Sawatzky, H. Verweij, Phys. Rev. Lett. 62 (1989) 221.
[8] D.A. Fischer, A.R. Moodenbaugh, Y. Xu, Physica C 215 (1995) 279.
[9] N. Merrien, F. Studer, C. Michel, P. Srivastava, B.R. Sekhar, N.L. Saini, K.B. Garg, G. Tourillon, J. Phys. Chem. Solids 54 (1993) 499.
[10] S.A. Warda, W. Pietzuch, G. Berghöfer, U. Kesper, W. Massa, D. Reinen, J. Solid State Chem. 138 (1998) 18, and references therein.
[11] R.A. Mohan Ram, K.K. Singh, W.H. Madhusudan, P. Ganguly, C.N.R. Rao, Mater. Res. Bull. 18 (1983) 703.
[12] G. Demazeau, B. Buffat, M. Pouchard, P. Hagenmüller, J. Solid State Chem. 54 (1984) 389.
[13] F.M.F. de Groot, J. Fuggle, B.T. Thole, G.A. Sawatzky, Phys. Rev. B 42 (1990) 5459.
[14] G. Kaindl, O. Strebel, A. Kolodziejczyk, W. Schäfer, R. Kiemel, S. Lösch, S. Kemmler-Sack, R. Hoppe, H.P. Müller, D. Kissel, Physica B 158 (1989) 446.
[15] M. Abbate, J.C. Fuggle, A. Fujimori, L.H. Tjeng, C.T. Chen, R. Potze, G. Sawatzky, H. Eisaki, S. Uchida, Phys. Rev. B 47 (1993) 16124.
[16] V.G. Bhide, D.S. Rajoria, Y.S. Reddy, G. Rama Rao, G.V. Subba Rao, C.N.R. Rao, Phys. Rev. Lett. 28 (1972) 1133.
[17] F.M.F. de Groot, Doctoral Thesis, Katholieke Universiteit Nijmegen, Nijmegen, 1991.
[18] T. Cowan, The Theory of Atomic Structure and Spectra, University of California Press, Berkeley, CA, 1981.
[19] P.H. Butler, Point Group Symmetry, Applications, Methods, and Tables, Plenum, New York, 1981.
[20] K. Okada, A. Kotani, B.T. Thole, J. Electron Spectrosc. Relat. Phenom. 58 (1997) 325.
[21] H. Eskes, G.A. Sawatzky, Phys. Rev. B 43 (1991) 119.
[22] M.A. van Veenendaal, H. Eskes, G.A. Sawatzky, Phys. Rev. B 47 (1993) 11462.
[23] J. Zaanen, G.A. Sawatzky, J.W. Allen, Phys. Rev. Lett. 55 (1985) 418.
[24] M. Atanasov, D. Reinen, J. Electron Spectrosc. Relat. Phenom. 86 (1997) 180.
[25] M. Abbate, R. Potze, G.A. Sawatzky, A. Fujimori, Phys. Rev. B 49 (1994) 7210.
[26] A. Fujimori, I. Hase, M. Nakamura, H. Namatame, Y. Fujishima, Y. Tokura, M. Abbate, F.M.F. de Groot, M.T. Czyzyk, J.C. Fuggle, O. Strebel, F. López, M. Domke, G. Kaindl, Phys. Rev. B 46 (1992) 9841.
[27] V.I. Anisimov, S.Yu. Ezhov, T.M. Rice, Phys. Rev. B 55 (1997) 12829.
[28] J. Fink, N. Nücker, E. Pellegrin, H. Romberg, M. Alexander, M. Knupfer, J. Electron. Spectrosc. Relat. Phenom. 66 (1994) 395.
[29] C. Sugiura, J. Chem. Phys. 58 (1972) 5444.
[30] C. Sugiura, T.J. Suzuki, J. Chem. Phys. 75 (1981) 4357.